Spectroscopic studies of anion complexes and clusters: A microscopic approach to understanding anion solvation

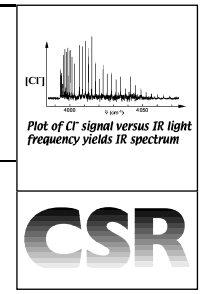

Evan J. Bieske

School of Chemistry, University of Melbourne, 3010 Australia. E-mail: evanjb@unimelb.edu.au

Received 28th November 2002
First published as an Advance Article on the web 9th May 2003

Recent infrared spectroscopic studies of negatively charged clusters in the gas phase have furnished new information on non-covalent bonds between anions and neutral molecules, and provided fresh perspectives on the microscopic details of anion solvation. We describe the central spectroscopic techniques employed for obtaining infrared spectra of mass-selected solvated anions in the gas phase, and illustrate recent progress by describing studies of simple halide-H_2 dimers, and larger clusters in which up to 9 C_2H_2 molecules are attached to a Cl^- anion.

1 Introduction

1.1 Overview

More than 30 years ago mass spectrometrists discovered that it is possible to prepare and isolate charged complexes and clusters in the gas-phase. When ions (*e.g.*, F^-, Cl^-) were introduced into a gas (*e.g.*, H_2O or CH_3CN vapour), it was observed that the neutral molecules tended to aggregate about the ions to form charged clusters (*e.g.*, F^-–$(H_2O)_n$ or Cl^-–$(CH_3CN)_n$).[1] It was soon recognized that these clusters, in which a "solute" ion is solvated by just a few "solvent" molecules, are appealing model systems for studying the interactions responsible for ion solvation in bulk media.[2] During the past 5 years, spectroscopists have learned how to collect and interpret vibrational spectra of negatively charged clusters. The spectra have provided new information on non-covalent bonds between anions and neutral molecules, and given us fresh perspectives on the microscopic details of anion solvation. In several ways anion complexes and clusters represent a frontier for gas-phase cluster spectroscopy. Although neutral, and more recently, positively charged complexes and clusters have been the subject of numerous spectroscopic investigations (see ref. 3), the corresponding negatively charged species have only recently proven amenable to spectroscopic characterisation.

Evan Bieske was born in Mackay, Australia. His interest in the spectroscopy of ions and ion clusters was initiated during his PhD studies, under the supervision of Professor A. E. W. Knight at Griffith University, Australia. Between 1990 and 1995 he worked as a postdoctoral fellow with Professor J. P. Maier in Basel, Switzerland, where he explored the properties of cation complexes and clusters through their electronic and infrared spectra. Since 1995, he has been at the University of Melbourne, where he has pursued spectroscopic investigations of mass-selected negatively charged complexes and clusters in the gas-phase.

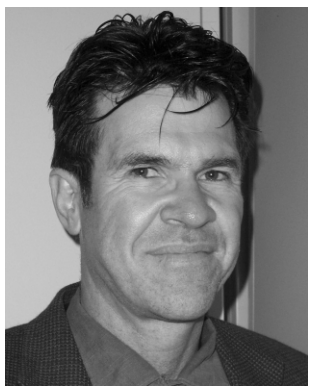

1.2 Motivations

Every chemist knows that anions are ubiquitous. Due to non-covalent electrostatic and induction forces, ions, wherever they exist, tend to be surrounded by a sheath of neutral solvent molecules. Solvation occurs not only in condensed media, but also in gaseous environments where anions seed the formation of negatively charged clusters. Generally, the solvent molecules play more than a spectator role and are crucial in influencing the chemical and physical properties of solute ions. For example, in the gas-phase the F^- ion is smaller than the Cl^- ion, and so the molar conductivity of F^- in aqueous solution might be expected to be larger than that of Cl^-. In fact, the molar conductivity of F^- is substantially *lower* than that of Cl^- (5.54 *vs* 7.635 mS m^2 mol^{-1}), the reason being that H_2O molecules bind very strongly to F^- so that as it moves, it is obliged to tow a large, cumbersome raft of water molecules.[4] The very effective solvation of F^- by water also accounts for its unreactive nature in aqueous solution compared to the gas-phase, and for the fact that HF is a stronger acid in aqueous solution than it would be otherwise. Small multiply charged anions, which are generally unstable in the absence of solvent molecules, represent another example where solvation plays a crucial role. Recently it has been shown that the SO_4^{2-} anion requires at least 3 solvent water molecules for it to be stable.[5]

1.3 Solvated ions in the gas phase

An essential precursor to explaining and predicting the behaviour of ions in solution is a thorough understanding of the way in which an ion interacts with a single solvent molecule (or a just few molecules). Experimental studies in this direction commenced in the 1960's when mass spectrometrists discovered that it was possible to prepare charged complexes consisting of neutral solvent molecules attached to an ion core.[2,6] This was followed by studies of clustering equilibria,

$$A^{\pm}–B_n + B \rightleftharpoons A^{\pm}–B_{n+1}$$

where $A^{\pm}$ is an atomic or molecular ion, and B is a 'solvent' atom or molecule. Measurements of the equilibrium constant over a range of temperatures allow van't Hoff plots to be constructed from which solvent binding enthalpies and entropies can be ascertained. Nowadays, the database for ion cluster energetics is vast, with the NIST WebBook containing ligand binding enthalpies and entropies for many thousands of

ion-neutral complexes.[7] Photoelectron spectroscopy, which involves measuring the energies of electrons photodetached by a fixed frequency laser beam, has also played a very significant, and more recent role in furnishing dissociation energies for anion-neutral intermolecular bonds.[8] While thermochemical and photoelectron studies are an excellent source of information on ion cluster energetics, they do not usually provide direct structural information (although abrupt declines in ligand binding energies often correspond to completion of a solvent shell; ref. 9).

1.4 Spectroscopy of anion complexes and clusters

More direct empirical information on the structures of anion clusters can be obtained from gas-phase spectra. Infrared spectroscopic investigations of gas-phase anion complexes commenced in the 1980's with studies of the FHF^- and $ClHCl^-$ bihalide anions (refs. 10 and 11). These species, which are held together by extremely strong hydrogen bonds, were interrogated using conventional techniques (diode laser absorption spectroscopy in a hollow cathode plasma discharge). More recently, beginning with a pioneering study of the study of the I^-–H_2O dimer,[12] resonant photofragmentation strategies have been deployed to record infrared spectra for more than 30 different anion cluster systems. Most of the characterised clusters consist of one or more "solvent" molecules containing an X–H group (*e.g.*, H_2, H_2O, C_2H_2, NH_3, CH_4, CH_3OH, C_2H_5OH) hydrogen-bonded to a core anion (*e.g.*, F^-, Cl^-, Br^-, I^-, O_2^-, SO_2^-). The halide–water clusters have received the most attention.[13,14,15,16] Hydrogen bonded anion clusters are attractive targets not only because of their chemical significance, but also because their hydrogen stretch vibrations can be excited by light in the 3 μm region that is readily generated by pulsed optical parametric oscillators.

Ideally, spectroscopic data can be used to develop, test and refine potential energy surfaces describing anion-neutral interactions. Readers interested in learning more about the connections between spectra of complexes and clusters and intermolecular potential energy surfaces should consult articles in four special issues of *Chemcial Reviews* (ref. 3). Spectra displaying rotationally resolved features provide relatively direct links to quantitative details of the intermolecular potential energy surface, since by analysing the rotational sub-structure it is possible to extract moments of inertia (from which one can deduce the arrangement of the constituent atoms), and estimate the bond force constants. Lower resolution spectra, displaying vibrational features, can often be used to distinguish between different possible isomeric forms, since the vibrational frequencies and intensities of the "solvent" molecules and "solute" ions depend sensitively upon their local environment.

The structure of small charged solute–solvent clusters depends upon the details of the solute–solvent and solvent–solvent interactions. Perhaps the simplest situation is encountered for complexes consisting of an atomic anion surrounded by rare gas (RG) atoms. In this case, the RG atoms are disposed about the anion, allowing the maximum number of RG-anion bonds to be formed. The RG atoms are in turn grouped in such a way that the number of weaker RG–RG bonds is maximized. This situation leads to interior solvation structures, and has been shown through photoelectron spectroscopy to apply to O^-–Ar_n[17] and I^-–Xe_n,[18] both of which exhibit solvent shell closure for $n = 12$, corresponding to icosohedral structures with a central anion.

Less obvious structures arise when the solvent–solvent and solute–solvent interactions are of comparable strengths. The most thoroughly explored examples are the halide–water clusters. Spectroscopic[13,14] and theoretical[15,16] studies show that when the larger halides (Cl^-, Br^-, I^-) are hydrated by a few water molecules, the clusters possess structures such that the halide resides on the surface of a H-bonded water network. The situation is different for F^-–$(H_2O)_n$; due to strong, directional $F^-\cdots HOH$ bonds, the water–water H-bonds are disrupted and F^- tends to occupy an interior solvation site.[19]

In the following sections we introduce the central experimental techniques used to obtain infrared spectra of anion complexes and clusters, and describe how the spectra can be interpreted to yield fundamental information on non-covalent interactions between anions and neutral molecules. As illustrative examples we concentrate on the Cl^-–H_2, Br^-–H_2, and I^-–H_2 dimers, and larger Cl^-–$(C_2H_2)_n$ clusters, where up to 9 acetylene molecules are attached to a Cl^- anion. For the simple halide–H_2 dimers, rotationally resolved infrared spectra provide the necessary information for deducing intermolecular separations, force constants for intermolecular bonds, and empirical intermolecular potential energy curves. Vibrationally resolved spectra of Cl^-–$(C_2H_2)_n$ clusters can be used to infer preferred solvation structures, and deduce how many C_2H_2 molecules are accommodated in the inner solvation shell.

2 Experimental approaches

2.1 Strategies for obtaining infrared spectra of anion clusters

Anion complexes and clusters are difficult species to study using standard spectroscopic methods. One problem is that in any plasma environment conducive to the formation of anion clusters, there are generally many different molecular species (including radicals and ions), that may absorb light over the same spectral range. For this reason, disentangling and assigning spectra can present severe difficulties. As well, usually it is difficult to create the clusters in sufficient densities for the implementation of traditional spectroscopic approaches (*e.g.*, direct infrared absorption spectroscopy).

A strategy with the requisite *selectivity* and *sensitivity*, involves exposing mass-selected ion complexes to tuneable infrared light in a tandem mass spectrometer, with photoabsorption being inferred through the production of charged photofragments. The scheme is illustrated, with application to the Cl^-–H_2 complex, in Fig. 1. In the first step, an IR photon

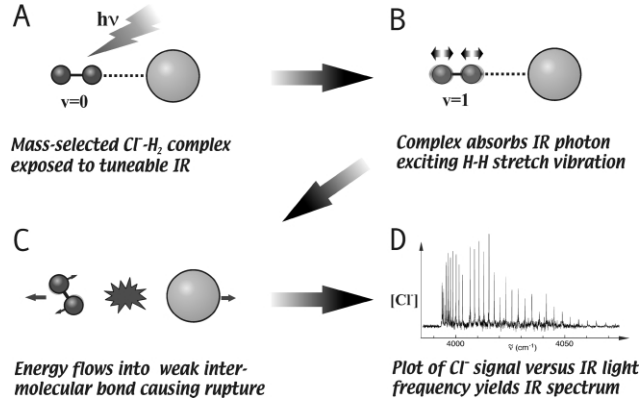

Fig. 1 Strategy for obtaining infrared VP spectra of mass-selected anion complexes applied to the Cl^-–H_2 dimer. An IR photon, with appropriate wavelength, excites the H–H stretch vibration. Energy migrates to the weak intermolecular bond, causing its rupture and liberation of a detectable Cl^- fragment.

excites a high frequency vibration (in this case the H–H stretch vibration), localised on one component of the complex. In the free H_2 molecule, the H–H stretch vibration is only very weakly infrared active; the vibrational transition is dipole forbidden but is weakly quadrupole allowed. However, the H–H stretch vibration becomes significantly infrared active when the H_2

molecule is attached to a halide anion. The energy in the H_2 stretch is eventually transferred to the weak intermolecular bond causing it to break. A spectrum is obtained by monitoring the charged Cl^- fragments as the infrared wavelength is scanned. The process by which vibrational energy flows into and breaks a weak bond, is known as *vibrational predissociation*, making it convenient to label the strategy as vibrational predissociation (VP) spectroscopy. This form of *action* spectroscopy is exquisitely sensitive, since charged particle detectors are able to sense single ions.

Target anion clusters are size-selected with a mass spectrometer prior to exposure to the IR beam, while fragment ions are size-selected in a second mass spectrometer stage. The great advantage of size selection for parents and offspring is that there is generally little doubt concerning the identity of the cluster ion being probed. Another significant benefit is that it is usually straightforward to obtain spectra of clusters containing increasing numbers of solvent molecules in order to explore the spectral consequences of the first few solvation steps. The VP strategy was first used in infrared studies of the H_3^+–$(H_2)_n$ clusters,[20] and has since been employed to characterise a variety of cation and anion clusters (see refs. 21 and 22).

One limitation of the VP approach is that it is only useful for probing transitions that terminate above the cluster's dissociation threshold (otherwise fragment ions are not produced). A trick for circumventing this difficulty entails synthesising and probing clusters containing a weakly bound "spy" atom (preferably a rare gas atom, such as Ar). Ideally, the "spy" atom does not perturb the vibrations of the "core" cluster, but is dislodged following absorption of infrared light, resulting in a fragment with a different mass than the parent anion cluster. This method has been deployed for probing hydrated halide anion complexes such as Cl^-–$(H_2O)_n$.[14] A second difficulty associated with the VP technique is that the upper levels are inevitably lifetime broadened because of coupling with the dissociative continuum. This is usually only a problem if line broadening exceeds the light source band-width (which for commercially available optical parametric oscillators ranges between 0.02 and 3 cm^{-1}).

2.2 Experimental arrangements

In our studies, the VP scheme is carried out using the tandem mass spectrometer system illustrated in Fig. 2. The apparatus consists of an ion source, primary quadrupole mass filter for selection of the parent ion clusters, an octopole ion guide (which serves to contain the ion beam), a secondary quadrupole mass filter for selection of the charged photofragments, and an ion detector. While travelling through the octopole guide, the ions encounter a counter-propagating IR beam, which when tuned to an appropriate wavelength, serves to excite the complexes to a predissociative vibrational level. Resulting anion photofragments are selected by a second quadrupole mass filter and subsequently sensed by a charged particle detector.

Anion clusters are synthesised by bombarding a gas mixture expanding from an orifice into a vacuum with electrons. The gas cools as it expands, reducing the temperature of the translational and rotational degrees of freedom to a few degrees K. The electron beam ionises the gas, forming a cooled micro-plasma. Halide anions (Cl^-, Br^-, I^-) are created through dissociative attachment of low energy electrons to appropriate precursor molecules ($CHCl_3$, CH_2Br_2, CH_3I) and combine with entrained neutral molecules (*e.g.*, H_2 and C_2H_2) through three-body association reactions.

3 Examples

3.1 The Cl^-–H_2, Br^-–H_2, I^-–H_2 anion dimers

3.1.1 Overview. As our first example we consider the Cl^-–H_2, Br^-–H_2, I^-–H_2 dimers, which have recently been investigated using infrared VP spectroscopy.[23–25] At this stage, these are the only weakly bound negatively charged complexes for which spectra displaying completely resolved rotational features have been obtained. As we shall see, the spectra provide quantitative information on the bonds between halide anions and H_2, the simplest neutral molecule.

The halide–H_2 dimers serve as useful model systems for assessing different theoretical strategies employed for generating potential energy surfaces of negatively charged complexes and clusters. Due to the diffuse nature of the excess charge, *ab initio* calculations for molecular anions and anion clusters are notoriously difficult (a discussion of *ab initio* calculations for anions can be found in ref. 26). For this reason it is essential that calculations are benchmarked against experimental data. Comparisons between experimental and theoretical data for systems such as Cl^-–$(H_2O)_n$ (refs. 14 and 16) and Cl^-–C_2H_2 (ref. 27), have usually focused on vibrational frequencies and ligand binding energies. Spectroscopic information for the halide–H_2 dimers, which includes vibrational frequencies, rotational and

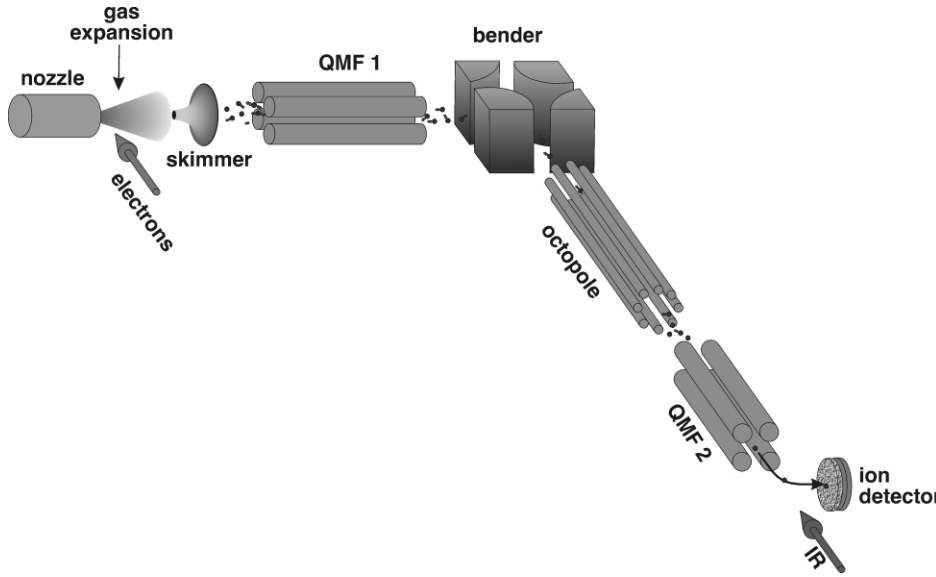

Fig. 2 Tandem mass spectrometer apparatus for spectroscopic investigations of anion clusters. The system is enclosed in a series of differentially pumped vacuum chambers.

centrifugal distortion constants, provides an extended data set against which *ab initio* computational strategies can be rigorously assessed.

Further motivation for studying the halide–H_2 complexes arises from their use as precursors in photoelectron studies designed to access the potential energy surfaces of fundamental triatomic rearrangement reactions.[28] For example, by photodetaching an electron from Cl^-–H_2, the system is projected onto the entrance channel region of the reaction:

$$Cl\ (^2P) + H_2 \rightarrow HCl + H$$

Although the halogen + H_2 reactions have been extensively studied, both experimentally and theoretically, several aspects remain unexplained. For example, contrary to observations for a large number of similar reactions, the non-adiabatic $Cl(^2P_{1/2})$ + H_2 channel is found to have a significantly larger cross section than the adiabatic $Cl(^2P_{3/2})$ + H_2 channel (for a discussion see ref. 29). Photoelectron spectra of the halide–H_2 complexes are most profitably interpreted to yield information on the neutral–neutral reactions, if the potential energy surfaces of the precursor anion complexes are known beforehand. This is just the sort of information that high resolution infrared studies are able to deliver.

3.1.2 Infrared spectra. Infrared VP spectra of the X^-–H_2 dimers in the H–H stretch region, are displayed in Fig. 3. What

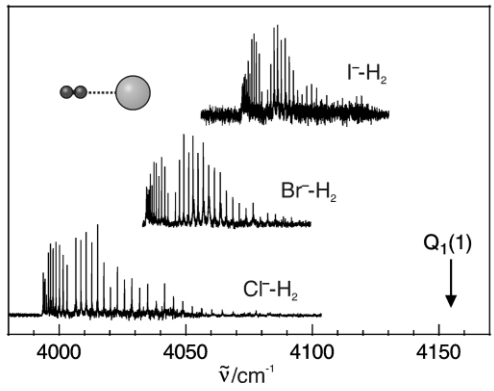

Fig. 3 Infrared spectrum of Cl^-–H_2, Br^-–H_2, and I^-–H_2 in the H–H stretch region. The bands, which are due to complexes containing *ortho* H_2, are shifted to lower frequency from the ($v = 1, j = 1$)←($v = 0, j = 1$) transition of H_2 (labelled $Q_1(1)$).

can the spectra tell us? First of all we note that the bands are shifted to lower frequency from the vibrational transition of the free H_2 molecule (which occurs at ≈4155 cm^{-1} for *ortho* H_2). The source of this vibrational shift can be understood by considering the complexes as intermediates for simple acid–base reactions in which a proton is transferred between hydride and halide anions:

$$H_2 + X^- \rightarrow H^- + HX$$

Since the proton affinity of H^- considerably exceeds those of Cl^-, Br^-, and I^-, the complexes have "reactant-like" forms. Nevertheless, in anticipation of proton transfer to the halide, the potential energy curve describing the H–H stretching vibration in the complexes is flatter than that of the free H_2 molecule, and as a consequence, the vibrational frequency for the H–H stretch is reduced compared to the free H_2 molecule. As expected, the vibrational shift tracks the proton affinity of the halide anions ($\Delta\nu_{Cl-} > \Delta\nu_{Br-} > \Delta\nu_{I-}$).

The distinctive rotational structure of the transitions shown in Fig. 3 (Σ–Σ bands, prominent P and R branches, and missing Q branch) suggests that the complexes possess linear equilibrium geometries, such that the H_2 molecule is H-bonded to the halide ion. This structure can be anticipated by considering the electrostatic interaction between the negatively charged halide and the H_2 quadrupole moment.

From the rotational and centrifugal constants (derived by analysing the spectra) one can estimate the intermolecular separations and harmonic force constants for the intermolecular bonds (assuming negligible distortion of the H_2 molecule). Vibrationally averaged separations between the halide and the midpoint of the H–H bond for Cl^-–H_2, Br^-–H_2, and I^-–H_2 are 3.20, 3.46, and 3.85 Å, while the force constants are 2.9, 1.9, and 1.3 N m^{-1}. The intermolecular bonds are rather long and weak, reflecting the fact that the constituents are bound together mainly by charge-quadrupole electrostatic and charge-induced-dipole induction interactions.

Vibrationally exciting the H_2 molecule has a profound effect on the intermolecular interaction. The P-branch heads, apparent in the spectra shown in Fig. 3, indicate that the intermolecular bonds contract when the H_2 molecule becomes vibrationally excited. The contraction, which for all three complexes is ≈0.1 Å, is accompanied by a corresponding increase in the stretching force constant for the intermolecular bond. The shortening and stiffening of the bonds are consequences of appreciable increases (≈10%) in the vibrationally averaged quadrupole moment and polarisabilities of the H_2 molecule when it is excited from $v = 0$ to $v = 1$.

3.1.3 *para*/*ortho* Effects. Normally H_2 gas is a mixture of 25% *para* H_2 modification (*even* rotational levels) and 75% *ortho* H_2 modification (*odd* rotational levels). Interconversion between *para* and *ortho* forms involves realignment of the H atom nuclear spins and is usually a very slow process. Although initially we expected to see distinguishable transitions for complexes containing *para*-H_2 and *ortho*-H_2, in fact, only transitions for complexes containing the *ortho* H_2 modification are apparent in the spectra shown in Fig. 3. There are two reasons for this. Firstly, for normal H_2 gas, the population ratio for *para* and *ortho* modifications is 1:3. Secondly, the Cl^-–$H_2(o)$ complex is more strongly bound than Cl^-–$H_2(p)$. This is because the lowest feasible dissociation route for Cl^-–$H_2(o)$ complexes involves production of H_2 fragments in the $j = 1$ rotational state (with energy $2B \approx 120$ cm^{-1} above the $j = 0$ state). For these two reasons, any Cl^-–$H_2(p)$ complexes formed in the ion source are efficiently converted to Cl^-–$H_2(o)$ through the exothermic ligand exchange reaction,

$$Cl^-\text{–}H_2(p) + H_2(o) \rightarrow Cl^-\text{–}H_2(o) + H_2(p)$$

To explore this issue, a spectrum of the Cl^-–D_2 isotopomer has been collected.[24] There is a better chance of observing complexes containing both modifications since, for D_2, the population ratio for the *even* and *odd* j levels is 2:1. Additionally, complexes containing *para* D_2 (*odd* j) are only bound by an additional ≈60 cm^{-1} compared to those containing *ortho* D_2 (*even* j). Indeed the spectrum of Cl^-–D_2, recorded in the region of the D–D stretch (Fig. 4), displays absorptions by Cl^-–$D_2(o)$ and Cl^-–$D_2(p)$, with the transitions separated by 0.24 cm^{-1}.

3.1.4 Halide–H_2 potential energy curves. The spectroscopic data can be used to develop effective radial potential energy curves describing the halide–H_2 intermolecular interactions. Near their minima, the potential curves are determined by Rydberg–Klein–Rees (RKR) inversion of the spectroscopic data.[24] At longer range, they are defined by the dominant electrostatic (charge-quadrupole) and induction (charge-induced-dipole) interactions, averaged over the hindered internal rotation of the H_2 sub-unit, assuming a Born–Oppenheimer type separation between the slow intermolecular stretch motion and the faster H–H stretch and intermolecular bend motions.

Radial potential energy curves for Cl^-, Br^-, and I^- interacting with *ortho* H_2 ($v = 0$) are plotted in Fig. 5. While at long range the curves are identical, they become noticeably

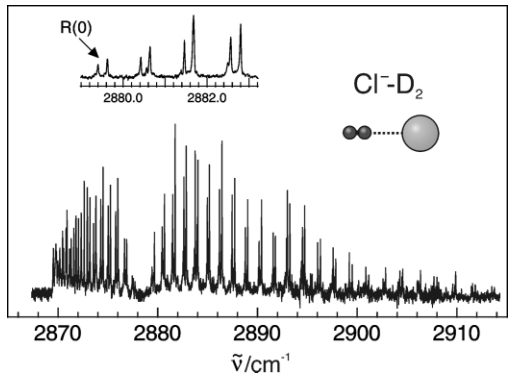

Fig. 4 Infrared VP spectrum of Cl^{-}–D_2 in the D–D stretch region. The inset is an expanded view of the first few R-branch lines, where doubling (Δ = 0.24 cm^{-1}) due to absorptions by complexes containing *ortho* and *para* D_2 is clearly evident.

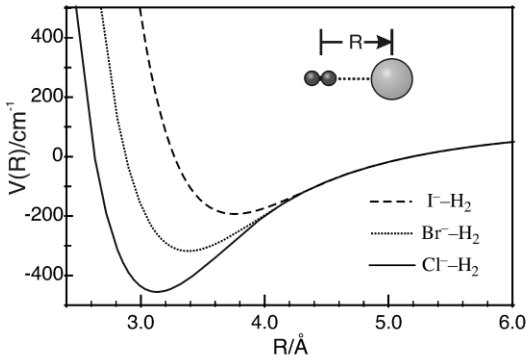

Fig. 5 Radial intermolecular potential energy curves for Cl^{-} + H_2, Br^{-} + H_2, and I^{-} + H_2. Near their minima, the potential curves are defined by RKR inversion of spectroscopic data, and at longer ranges by the electrostatic and inductions interactions between the H_2 and halide anion.

shallower and have a larger equilibrium separation as the size of the halide ion increases. Dissociation energies for Cl^{-}–H_2 (*o*), Br^{-}–H_2 (*o*), and I^{-}–H_2 (*o*) are 488, 365 and 253 cm^{-1}, confirming that the complexes are indeed fragile species.

3.2 Chloride–acetylene clusters

3.2.1 Overview. Our second example concerns clusters that are comprised of acetylene molecules attached to a chloride anion.[30] Although the spectra do not display rotationally resolved features, it is possible to deduce cluster structures by following the evolution of the vibrational bands as the clusters become larger. It turns out that the smaller clusters have highly symmetrical conformations in which equivalent acetylene molecules are H-bonded to a central Cl^{-} anion. For larger clusters, the spectra provide evidence for the existence of acetylene molecules in the second solvation shell, and for multiple coexisting isomeric forms.

Before examining the infrared spectra, it is worthwhile considering how a single acetylene molecule binds to a Cl^{-} anion. The dominant long-range force acting between Cl^{-} and an acetylene molecule arises from the electrostatic interaction between the negative charge on the halide and quadrupole moment on the acetylene molecule. This favours a linear, H-bonded structure, which is also the one predicted by *ab initio* calculations.[27]

The infrared spectra are measured in the C–H stretch region and so it is also important to consider the effect of the attached halide on the symmetric (ν_1) and antisymmetric (ν_3) C–H stretch vibrations of the C_2H_2 molecule. The C–C stretch and bending vibrations lie below the spectral range of the IR light source and can be disregarded for the moment. As illustrated in Fig. 6, formation of a linear H-bond leads to a transformation of

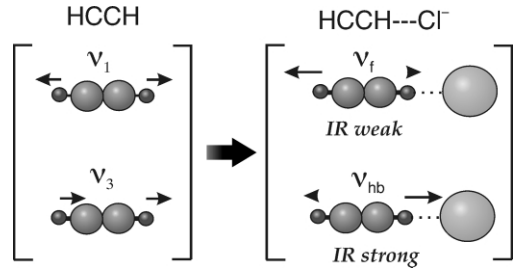

Fig. 6 Transformation of the symmetric (ν_1) and antisymmetric (ν_3) C–H stretch vibrations of C_2H_2 into hydrogen bonded (ν_{HB}) and a free (ν_F) C–H stretches in the Cl^{-}–C_2H_2 complex.

the ν_1 and ν_3 C–H stretch vibrations of the free C_2H_2 molecule into vibrational modes that mainly involve motion of the H-bonded and free C–H groups. The free C–H stretch vibration (ν_F) is predicted have a frequency that lies between those of the free C_2H_2 molecules' ν_1 and ν_3 stretches and is associated with a very weak infrared transition. In contrast, the H-bonded C–H stretch vibration (ν_{HB}) is predicted to be shifted substantially to lower frequency from the C–H stretches of the free C_2H_2 molecule (a red shift) and to be enhanced in infrared intensity. The red shift and infrared intensity both increase with the strength of the H-bond.

3.2.2 Infrared spectra. Infrared spectra of mass selected Cl^{-}–$(C_2H_2)_n$ clusters, taken over the range spanning the C–H stretch vibrations, are shown in Fig. 7. Clusters containing two

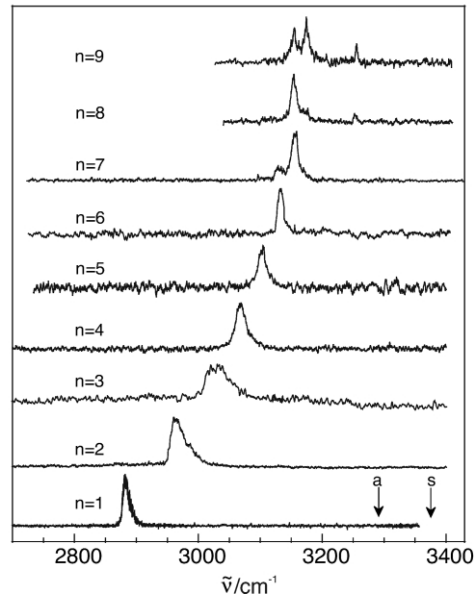

Fig. 7 Infrared VP spectra of Cl^{-}–$(C_2H_2)_n$ n = 1–9 anion complexes over the 2700–3420 cm^{-1} range. The arrows labelled "s" and "a" mark the ν_1 and ν_3 vibrations of bare C_2H_2.

or more acetylene molecules were created and probed by monitoring Cl^{-}–$(C_2H_2)_{n-1}$ photofragments for n = 2–5, and Cl^{-}–$(C_2H_2)_{n-2}$ photofragments for n = 6–9. It was not possible to obtain the spectrum of the cold Cl^{-}–C_2H_2 dimer directly because the Cl^{-}–C_2H_2 bond energy is so large that absorption of a single infrared photon does not result in photodissociation. Instead, Cl^{-}–C_2H_2.Ar complexes were formed and monitored through production of Cl^{-}–C_2H_2 fragments. The attached Ar atom is expected to have a minor influence on the vibrational frequencies of the core Cl^{-}–C_2H_2 dimer.

The infrared peak for the Cl^-–C_2H_2 dimer occurs at ≈ 2880 cm^{-1}, well below the antisymmetric and symmetric C–H stretch vibrations of the free acetylene molecule, good evidence that the dimer indeed possesses a linear H-bonded structure, as predicted by *ab initio* calculations.[27] What happens as more acetylene molecules are added? As seen in Fig. 7, for clusters containing up to 6 C_2H_2 molecules, the spectra are remarkably simple, each containing a single, compact band. This suggests that clusters of a particular size have a single isomeric form, in which equivalent acetylene molecules are bound end-on to the chloride anion. The bands' regular shift to higher frequency as more C_2H_2 molecules are added, implies that the chloride–acetylene bonds diminish steadily in strength as the clusters become larger. The C_2H_2 molecules should avoid one another (due to repulsive quadrupole–quadrupole interactions), resulting in structures reminiscent of those commonly encountered for inorganic metal–ligand complexes (Fig. 8). The clusters are

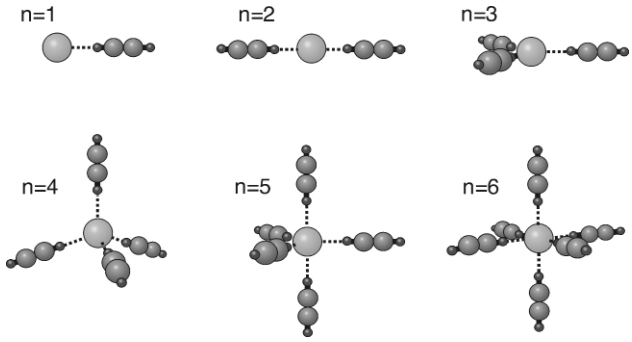

Fig. 8 Proposed structures for the Cl^-–$(C_2H_2)_n$ n = 1–6 clusters.

expected to be extremely floppy, undergoing substantial zero point excursions, particularly in vibrational modes corresponding to angular motion of the C_2H_2 ligands about the Cl^- core.

3.2.3 The second solvation shell and coexisting isomers. The Cl^-–$(C_2H_2)_n$ spectra undergo a remarkable change for clusters containing more than 6 acetylene molecules. To provide a clearer view, the n = 6–9 spectra are plotted on an expanded scale in Fig. 9. Clearly, the n = 7–9 spectra display

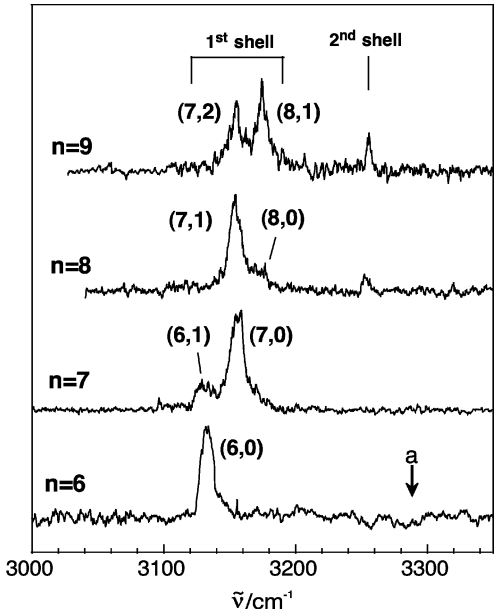

Fig. 9 Infrared spectra of the Cl^-–$(C_2H_2)_n$ n = 6–9 complexes. The arrow labelled "a" marks the ν_3 band of bare C_2H_2.

multiple bands, evidence that the clusters contain inequivalent acetylene sub-units. The spectra exhibit several features that assist in their interpretation. In the n = 8 and 9 spectra there is an isolated peak, much closer to the ν_3 absorption of free C_2H_2. This peak, which is absent in the spectra of the smaller clusters, is due to an acetylene molecule (or acetylene molecules) that is not directly bonded to the Cl^- anion, but which is situated in the second solvation shell.

The multiple peaks lying to lower energy in the n = 7–9 spectra are due to acetylene molecules in the inner solvation shell. The smaller peak in the n = 7 spectrum, which occurs at the same position as the n = 6 peak can be connected with a (6,1) isomer with six C_2H_2 molecules in the first solvation shell and one in the second. The larger peak is associated with a (7,0) isomer in which 7 equivalent acetylenes are directly attached to the Cl^-. The n = 8 spectrum can be interpreted in an analogous way; the strongest peak occurs at the same position as the (7,0) peak and can be assigned to a (7,1) isomer, while the small shoulder at 3173 cm^{-1} can be associated with an (8,0) isomer. In a similar way, the n = 9 spectrum can be interpreted in terms of coexisting (7,2) and (8,1) isomers.

What do the larger clusters look like, and where are the second solvation shell acetylenes situated? Although, at this stage it is impossible to definitely answer these questions, we can take a guess by considering the long-range intermolecular forces. The dominant cohesive forces for C_2H_2 molecules in the second solvation shell arise from charge-quadrupole and induction interactions with the central Cl^-, both of which favor end-on approach of the second solvation shell ligand. This, together with the fact that the acetylene–acetylene potential favors a slipped parallel arrangement for the acetylene dimer, means that the additional ligands are likely to slip end-on between inner shell acetylenes, while being prevented from making intimate contact with the Cl^- core because of steric crowding. Based on these considerations, two isomeric forms of Cl^-–$(C_2H_2)_7$ are shown in Fig. 10.

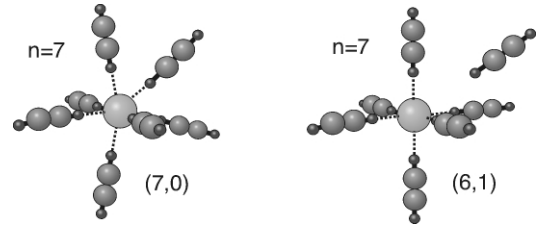

Fig. 10 Two isomer clusters for Cl^-–$(C_2H_2)_7$, one in which all 7 C_2H_2 units are directly H-bonded to the Cl^-, and the other with one C_2H_2 unit in the second solvation shell.

4 Conclusions and outlook

In this brief overview we have described how infrared spectra of negatively charged complexes and clusters in the gas-phase can be obtained and interpreted to derive structural information and potential energy surfaces describing interactions between anions and neutral molecules. So far, a somewhat restricted range of anion clusters have been characterised, and for the most part the spectra exhibit vibrational, rather than rotational resolution. The future will undoubtedly see the application of existing techniques to previously uncharacterised species, and the development and deployment of new strategies. It is particularly desirable to record rotationally resolved spectra of the hydrated-halide dimers so that reliable potential energy surfaces, applicable for describing aqueous solvation of halide anions, can be developed. This is a challenging enterprise, since the strong halide–water bonds mean that it is impossible to apply the VP strategy directly. As noted earlier, significant progress has been made in gathering vibrational data for the hydrated-halides by attaching Ar "spy" atoms that are dislodged following photo-excitation of a high frequency vibration. The

problem is that one forgoes the chance of obtaining high-resolution spectra for the core anion complex. On the positive side, the relatively strong intermolecular bonds may favour their formation in sufficient abundances for investigation using traditional spectroscopic techniques such as direct infrared absorption in electron-impact excited supersonic plasmas (as described in ref. 31, this approach has been used for cation complexes such as $Ar–HN_2^+$ and N_4^+)

So far, spectroscopic investigations of negatively charged complexes and clusters have been confined to the mid-infrared part of the spectrum (2500–4500 cm^{-1}). One promising approach to extending the spectral range, demonstrated in recent studies of $Br^–(HBr)_n$ clusters,[32] entails probing anion clusters with the IR output of a free electron laser, which produces an intense burst of 1 ps micropulses, tuneable below 2000 cm^{-1}. This is the spectral region in which X–H groups engaged in very strong hydrogen bonds absorb, and which is currently inaccessible to optical parametric oscillators. Generally, absorption of several of the lower energy IR photons is necessary before the complexes have sufficient energy to dissociate and produce a detectable ion fragment. Electronic spectroscopy has not played a significant role in anion cluster spectroscopy; indeed many anions do not possess excited electronic states lying below the electron detachment threshold. Nor has microwave spectroscopy been applied to probe anion complexes and clusters, although its successful application to characterise cation complexes (*e.g.*, $Ar–HCO^+$, ref. 33) suggests that studies are certainly possible.

5 Acknowledgements

The Australian Research Council and the University of Melbourne are acknowledged for their generous support. Contributions by D. A. Wild, Z. M. Loh, and R. L. Wilson to the anion spectroscopic investigations at the University of Melbourne are gratefully recognised.

6 References

1 P. Kebarle, M. Arshadi and J. Scarborough, *J. Chem. Phys.*, 1968, **49**, 817.
2 A. W. Castleman and R. G. Keesee, *Chem. Rev.*, 1986, **86**, 589.
3 Four thematic issues of *Chemical Reviews* [Vol. 86, No.3 (1986); Vol. 88, No. 6 (1988); Vol. 94, No. 7 (1994); Vol. 100, No. 11, (2000)] are devoted to van der Waals complexes and clusters.
4 P. W. Atkins and J. de Paula, *Physical Chemistry*, Oxford University Press, Oxford, UK, 2002.
5 X. Yang, X.-B. Wang and L.-S. Wang, *J. Phys. Chem. A*, 2002, **106**, 7607.
6 P. Kebarle, *Ann. Rev. Phys. Chem.*, 1977, **28**, 445.
7 M. M. Meot-Ner and S. G. Lias, 'Binding Energies Between Ions and Molecules and The Thermochemistry of Cluster Ions', in *NIST Chemistry WebBook, NIST Standard Reference Database Number 69*, ed. P. J. Linstrom and W. G. Mallard, National Institute of Standards and Technology, Gaithersburg MD, 20899 (http://webbook.nist.gov), 2002.
8 A. W. Castleman, Jr. and K. H. Bowen, Jr., *J. Phys. Chem.*, 1996, **100**, 12911.
9 M. Meot-Ner and C. V. Speller, *J. Phys. Chem.*, 1986, **90**, 6616.
10 K. Kawaguchi and E. Hirota, *J. Chem. Phys.*, 1987, **87**, 6838.
11 K. Kawaguchi, *J. Chem. Phys.*, 1988, **88**, 4186.
12 M. S. Johnson, K. T. Kuwata, C.-K. Wong and M. Okumura, *Chem. Phys. Lett.*, 1996, **260**, 551.
13 P. Ayotte, G. H. Weddle, J. Kim, J. Kelley and M. A. Johnson, *J. Phys. Chem. A*, 1999, **103**, 443.
14 P. Ayotte, G. H. Weddle and M. A. Johnson, *J. Chem. Phys.*, 1999, **110**, 7129.
15 J. E. Combariza, N. R. Kestner and J. Jortner, *J. Chem. Phys.*, 1994, **100**, 2851.
16 S. S. Xantheas, *J. Phys. Chem.*, 1996, **100**, 9703.
17 S. T. Arnold, J. H. Hendricks and K. H. Bowen, *J. Chem. Phys.*, 1995, **102**, 39.
18 T. Lenzer, M. R. Furlanetto, N. L. Pivonka and D. M. Neumark, *J. Chem. Phys.*, 1999, **110**, 6714.
19 O. M. Cabarcos, C. J. Weinheimer, J. M. Lisy and S. S. Xantheas, *J. Chem. Phys.*, 1999, **110**, 5.
20 M. Okumura, L. I. Yeh and Y. T. Lee, *J. Chem. Phys.*, 1985, **83**, 3705.
21 M. A. Duncan, *Int. J. Mass Spectrom.*, 2000, **200**, 545.
22 E. J. Bieske and O. Dopfer, *Chem. Rev.*, 2000, **100**, 3963.
23 D. A. Wild, R. L. Wilson, P. S. Weiser and E. J. Bieske, *J. Chem. Phys.*, 2000, **113**, 10154.
24 D. A. Wild, P. S. Weiser, E. J. Bieske and A. Zehnacker, *J. Chem. Phys.*, 2001, **115**, 824.
25 D. A. Wild, Z. M. Loh, R. L. Wilson and E. J. Bieske, *J. Chem. Phys.*, 2002, **117**, 3256.
26 J. Simons and K. H. Jordan, *Chem. Rev.*, 1987, **87**, 535.
27 P. Botschwina and R. Oswald, *J. Chem. Phys.*, 2002, **117**, 4800.
28 D. M. Neumark, *PhysChemComm*, 2002, **5**, 76.
29 F. Dong, S.-H. Lee and K. Liu, *J. Chem. Phys.*, 2001, **115**, 1197.
30 P. S. Weiser, D. A. Wild and E. J. Bieske, *J. Chem. Phys.*, 1999, **110**, 9443.
31 H. Linnartz, D. Verdes and T. Speck, *Rev. Sci. Instr.*, 2000, **71**, 1811.
32 N. L. Pivonka, C. Kaposta, G. von Helden, G. Meijer, L. Wöste, D. M. Neumark and K. R. Asmis, *J. Chem. Phys.*, 2002, **117**, 6493.
33 Y. Ohshima, Y. Sumiyoshi and Y. Endo, *J. Chem. Phys.*, 1997, **106**, 2977.